Chapter 6

Optical Properties of Solids Over a Wide Frequency Range

6.1 Kramers–Kronig Relations

References

- Yu and Cardona, Fundamentals of Semiconductors, Springer Verlag (1996). §6.1.3 and §6.6.

- Jones and March, *Theoretical Solid State Physics*: pp. 787-793

- Jackson, *Classical Electrodynamics*: pp. 306-312

Measurement of the absorption coefficient (Chapter 11) gives the imaginary part of the complex index of refraction, while the reflectivity is sensitive to a complicated combination of $\varepsilon_1(\omega)$ and $\varepsilon_2(\omega)$. Thus from measurements such as $\alpha_{\mathrm{abs}}(\omega)$ we often have insufficient information to determine $\varepsilon_1(\omega)$ and $\varepsilon_2(\omega)$ independently. However, if we know either $\varepsilon_1(\omega)$ or $\varepsilon_2(\omega)$ over a wide frequency range, then $\varepsilon_2(\omega)$ or $\varepsilon_1(\omega)$ can be determined from the Kramers–Kronig relation given by

$$\varepsilon_1(\omega) - 1 = \frac{2}{\pi}\mathcal{P}\int_0^\infty \frac{\omega'\varepsilon_2(\omega')}{\omega'^2 - \omega^2}d\omega' \tag{6.1}$$

and

$$\varepsilon_2(\omega) = -\frac{2}{\pi}\mathcal{P}\int_0^\infty \frac{\omega'\varepsilon_1(\omega')}{\omega'^2 - \omega^2}d\omega' \tag{6.2}$$

in which $\mathcal{P}$ denotes the principal value. The Kramers–Kronig relations are based on causality, linear response theory and the boundedness of physical observables.

The Kramers–Kronig relations relate $\varepsilon_1(\omega)$ and $\varepsilon_2(\omega)$ so that if either of these functions is known as a function of ω the other is completely determined. Because of the form of these relations (Eqs. 6.1 and 6.2), it is clear that the main contribution to $\varepsilon_1(\omega)$ comes from the behavior of $\varepsilon_2(\omega')$ near $\omega' \approx \omega$ due to the resonant denominator in these equations. What this means is that to obtain $\varepsilon_1(\omega)$, we really should know $\varepsilon_2(\omega')$ for all ω', but it is more important to know $\varepsilon_2(\omega')$ in the frequency range about ω than elsewhere. This property is greatly exploited in the analysis of reflectivity data, where measurements are available

over a finite range of ω' values. Some kind of extrapolation procedure must be used for those frequencies ω' that are experimentally unavailable. We now give a derivation of the Kramers–Kronig relations after some introductory material.

This theorem is generally familiar to electrical engineers in another context. If a system is linear and obeys causality (i.e., there is no output before the input is applied), then the real and imaginary parts of the system function are related by a Hilbert transform. Let us now apply this causality concept to the polarization in a solid resulting from the application of an optical electric field. We have the constitutive equation which defines the polarization of the solid:

$$\varepsilon \vec{E} = \vec{D} = \vec{E} + 4\pi \vec{P} \tag{6.3}$$

so that

$$\vec{P} = \frac{\varepsilon - 1}{4\pi} \vec{E} \equiv \alpha(\omega) \vec{E} \tag{6.4}$$

where $\alpha(\omega)$ defines the polarizability, and $\vec{P}$ is the polarization/unit volume or the response of the solid to an applied field $\vec{E}$. The polarizability $\alpha(\omega)$ in electrical engineering language is the system function

$$\alpha(\omega) = \alpha_r(\omega) + i\alpha_i(\omega) \tag{6.5}$$

in which we have explicitly written the real and imaginary parts $\alpha_r(\omega)$ and $\alpha_i(\omega)$, respectively. Let $E(t) = E_0 \delta(t)$ be an impulse field at $t = 0$. Then from the definition of a δ-function, we have:

$$E(t) = E_0 \delta(t) = \frac{E_0}{\pi} \int_{0^-}^{\infty} \cos \omega t \, d\omega. \tag{6.6}$$

The response to this impulse field yields an in-phase term proportional to $\alpha_r(\omega)$ and an out-of-phase term proportional to $\alpha_i(\omega)$, where the polarization vector is given by

$$\vec{P}(t) = \frac{E_0}{\pi} \int_{0^-}^{\infty} \left[\alpha_r(\omega) \cos \omega t + \alpha_i(\omega) \sin \omega t \right] d\omega, \tag{6.7}$$

in which $\alpha(\omega)$ is written for the complex polarizability (see Eq. 6.5). Since $\vec{P}(t)$ obeys causality and is bounded, we find that the integral of $\alpha(\omega)e^{-i\omega t}$ is well behaved along the contour C' as $R \to \infty$ and no contribution to the integral is made along the contour C' in the upper half plane (see Fig. 6.1). Furthermore, the causality condition that $\vec{P}(t)$ vanishes for $t < 0$ requires that $\alpha(\omega)$ have no poles in the upper half plane shown in Fig. 6.1.

To find an explicit expression for $\alpha(\omega)$ we must generate a pole on the real axis. Then we can isolate the behavior of $\alpha(\omega)$ at some point ω_0 by taking the principal value of the integral. We do this with the help of Cauchy's theorem. Since $\alpha(\omega)$ has no poles in the upper half-plane, the function $[\alpha(\omega)/(\omega - \omega_0)]$ will have a single pole at $\omega = \omega_0$ (see Fig. 6.2). If we run our contour just above the real axis, there are no poles in the upper-half plane and the integral around the closed contour vanishes:

$$\oint \frac{\alpha(\omega) d\omega}{\omega - \omega_0} = 0. \tag{6.8}$$

Let us now consider the integral taken over the various portions of this closed contour:

$$\int_{C'} \frac{\alpha(\omega)}{\omega - \omega_0} d\omega + \int_{-R}^{\omega_0 - \epsilon} \frac{\alpha(\omega)}{\omega - \omega_0} d\omega + \int_{C} \frac{\alpha(\omega)}{\omega - \omega_0} d\omega + \int_{\omega_0 + \epsilon}^{R} \frac{\alpha(\omega) d\omega}{\omega - \omega_0} = 0. \tag{6.9}$$
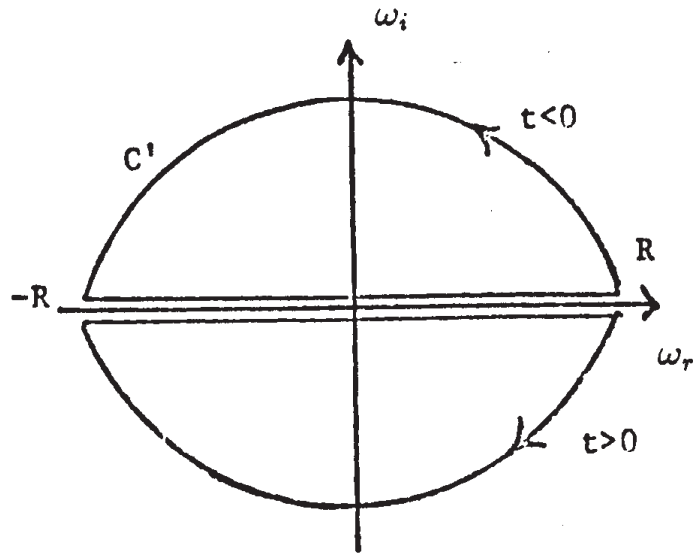
59

Figure 6.1: Contours used in evaluating the complex polarizability integral of Eq. 6.7.
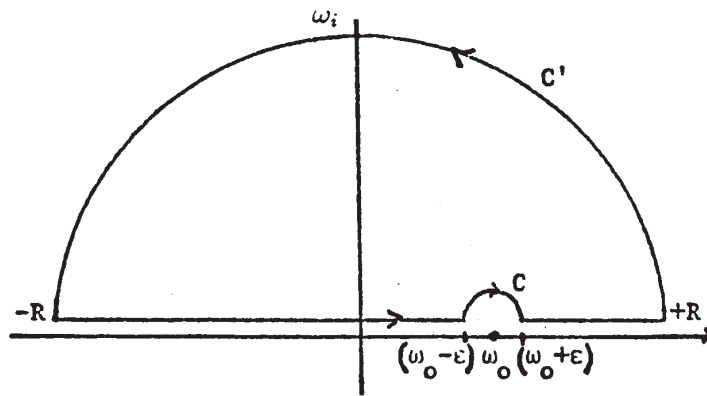

Figure 6.2: Contour used to evaluate Eq. 6.9.

60

The contribution over the contour C' vanishes since $\alpha(\omega)$ remains bounded, while $\frac{1}{\omega - \omega_0} \to 0$ as $R \to \infty$ (see Fig. 6.2). Along the contour C, we use Cauchy's theorem to obtain

$$\lim_{\epsilon \to 0} \int_C \frac{\alpha(\omega)}{\omega - \omega_0} d\omega = -\pi i \alpha(\omega_0) \tag{6.10}$$

in which $\alpha(\omega_0)$ is the residue of $\alpha(\omega)$ at $\omega = \omega_0$ and the minus sign is written because the contour C is taken clockwise. We further define the principal part $\mathcal{P}$ of the integral in the limit $R \to \infty$ and $\epsilon \to 0$ as

$$\lim_{\substack{R \to \infty \\ \epsilon \to 0}} \int_{-R}^{\omega_0 - \varepsilon} \frac{\alpha(\omega)}{\omega - \omega_0} d\omega + \int_{\omega_0 + \epsilon}^{R} \frac{\alpha(\omega)}{\omega - \omega_0} d\omega \to \mathcal{P} \int_{-\infty}^{\infty} \frac{\alpha(\omega)}{\omega - \omega_0} d\omega. \tag{6.11}$$

The vanishing of the integral in Eq. 6.8 thus results in the relation

$$\alpha_r(\omega_0) + i\alpha_i(\omega_0) = \frac{1}{\pi i} \mathcal{P} \int_{-\infty}^{\infty} \frac{\alpha_r(\omega) + i\alpha_i(\omega)}{\omega - \omega_0} d\omega. \tag{6.12}$$

Equating real and imaginary parts of Eq. 6.12, we get the following relations which hold for $-\infty < \omega < \infty$;

$$\alpha_r(\omega_0) = \frac{1}{\pi} \mathcal{P} \int_{-\infty}^{\infty} \frac{\alpha_i(\omega)}{\omega - \omega_0} d\omega \tag{6.13}$$

where $\alpha_r(\omega)$ is even and

$$\alpha_i(\omega_0) = \frac{-1}{\pi} \mathcal{P} \int_{-\infty}^{\infty} \frac{\alpha_r(\omega)}{\omega - \omega_0} d\omega \tag{6.14}$$

where $\alpha_i(\omega)$ is odd.

We would like to write these relations in terms of integrals over positive frequencies. We can do this by utilizing the even- and oddness of $\alpha_r(\omega)$ and $\alpha_i(\omega)$. If we now multiply the integrand by $(\omega + \omega_0)/(\omega + \omega_0)$ and make use of the even- and oddness of the integrands, we get:

$$\alpha_r(\omega_0) = \frac{1}{\pi} \mathcal{P} \int_{-\infty}^{\infty} \frac{\alpha_i(\omega)(\omega + \omega_0)}{\omega^2 - \omega_0^2} d\omega = \frac{2}{\pi} \mathcal{P} \int_{0}^{\infty} \frac{\omega \alpha_i(\omega) d\omega}{\omega^2 - \omega_0^2} \tag{6.15}$$

$$\alpha_i(\omega_0) = \frac{-1}{\pi} \mathcal{P} \int_{-\infty}^{\infty} \frac{\alpha_r(\omega)(\omega + \omega_0)}{\omega^2 - \omega_0^2} d\omega = -\frac{2}{\pi} \mathcal{P} \int_{0}^{\infty} \frac{\omega_0 \alpha_r(\omega) d\omega}{\omega^2 - \omega_0^2}. \tag{6.16}$$

We have now obtained the Kramers–Kronig relations. To avoid explicit use of the principal value of a function, we can subtract out the singularity at ω_0, by writing

$$\alpha_r(\omega_0) + i\alpha_i(\omega_0) = \frac{1}{\pi i} \int_{-\infty}^{\infty} \left(\frac{\alpha(\omega) - \alpha(\omega_0)}{\omega - \omega_0} \right) \left(\frac{\omega + \omega_0}{\omega + \omega_0} \right) d\omega. \tag{6.17}$$

Using the evenness and oddness of $\alpha_r(\omega)$ and $\alpha_i(\omega)$ we then obtain

$$\alpha_r(\omega_0) = \frac{2}{\pi} \int_{0}^{\infty} \frac{\omega \alpha_i(\omega) - \omega_0 \alpha_i(\omega_0)}{\omega^2 - \omega_0^2} d\omega \tag{6.18}$$

and

$$\alpha_i(\omega_0) = -\frac{2}{\pi} \int_{0}^{\infty} \frac{\omega_0 \alpha_r(\omega) - \omega_0 \alpha_r(\omega_0)}{\omega^2 - \omega_0^2} d\omega. \tag{6.19}$$

61

To obtain the Kramers–Kronig relations for the dielectric function itself, just substitute

$$\varepsilon(\omega) = 1 + 4\pi\alpha(\omega) = \varepsilon_1(\omega) + i\varepsilon_2(\omega) \tag{6.20}$$

to obtain

$$\varepsilon_1(\omega_0) - 1 = \frac{2}{\pi} \int_0^\infty \frac{\omega'\varepsilon_2(\omega') - \omega_0\varepsilon_2(\omega_0)}{\omega'^2 - \omega_0^2} d\omega' \tag{6.21}$$

$$\varepsilon_2(\omega_0) = \frac{-2}{\pi} \int_0^\infty \frac{\omega_0\varepsilon_1(\omega') - \omega_0\varepsilon_1(\omega_0)}{\omega'^2 - \omega_0^2} d\omega'. \tag{6.22}$$

The Kramers–Kronig relations are very general and depend, as we have seen, on the assumptions of causality, linearity and boundedness. From this point of view, the real and imaginary parts of a "physical" quantity Q can be related by making the identification

$$Q_{\text{real}} \rightarrow \alpha_r \tag{6.23}$$

$$Q_{\text{imaginary}} \rightarrow \alpha_i. \tag{6.24}$$

Thus, we can identify $\varepsilon_1(\omega) - 1$ with $\alpha_r(\omega)$, and $\varepsilon_2(\omega)$ with $\alpha_i(\omega)$. The reason, of course, why the identification $\alpha_r(\omega)$ is made with $[\varepsilon_1(\omega) - 1]$ rather than with $\varepsilon_1(\omega)$ is that if $\varepsilon_2(\omega) \equiv 0$ for all ω, we want $\varepsilon_1(\omega) \equiv 1$ for all ω (the dielectric constant for free space).

Thus, if we are interested in constructing a Kramers–Kronig relation for the optical constants, then we again want to make the following identification for the optical constants $(\tilde{n} + i\tilde{k})$

$$[\tilde{n}(\omega) - 1] \rightarrow \alpha_r(\omega) \tag{6.25}$$

$$\tilde{k}(\omega) \rightarrow \alpha_i(\omega). \tag{6.26}$$

From Eqs. 6.21 and 6.22, we can obtain the Kramers–Kronig relations for the optical constants $\tilde{n}(\omega)$ and $\tilde{k}(\omega)$

$$\tilde{n}(\omega) - 1 = \frac{2}{\pi} \int_0^\infty \frac{\omega'\tilde{k}(\omega') - \omega\tilde{k}(\omega)}{\omega'^2 - \omega^2} d\omega' \tag{6.27}$$

and

$$\tilde{k}(\omega) = -\frac{2}{\pi} \int_0^\infty \frac{\omega\tilde{n}(\omega') - \omega\tilde{n}(\omega)}{\omega'^2 - \omega^2} d\omega' \tag{6.28}$$

where we utilize the definition relating the complex dielectric function $\varepsilon(\omega)$ to the optical constants $\tilde{n}(\omega)$ and $\tilde{k}(\omega)$ where $\varepsilon(\omega) = [\tilde{n}(\omega) + i\tilde{k}(\omega)]^2$.

It is useful to relate the optical constants to the reflection coefficient $r(\omega)\exp[i\theta(\omega)]$ defined by

$$r(\omega)\exp[i\theta(\omega)] = \frac{\tilde{n}(\omega) - 1 + i\tilde{k}(\omega)}{\tilde{n}(\omega) + 1 + i\tilde{k}(\omega)} \tag{6.29}$$

in which the conjugate variables are $\ln r(\omega)$ and $\theta(\omega)$ and the reflectivity is given as $\mathcal{R}(\omega) = r^2(\omega)$. From Eq. 6.29, we can then write

$$\tilde{n}(\omega) = \frac{1 - r^2(\omega)}{1 + r^2(\omega) - 2r(\omega)\cos\theta(\omega)} \tag{6.30}$$

$$\tilde{k}(\omega) = \frac{2r(\omega)\sin\theta(\omega)}{1 + r^2(\omega) - 2r(\omega)\cos\theta(\omega)} \tag{6.31}$$

so that once $r(\omega)$ and $\theta(\omega)$ are found, the optical constants $\tilde{n}(\omega)$ and $\tilde{k}(\omega)$ are determined. In practice $r(\omega)$ and $\theta(\omega)$ are found from the reflectivity $\mathcal{R}$ which is measured over a wide frequency range and is modeled outside the measured range. A Kramers–Kronig relation can be written for the conjugate variables $\ln r(\omega)$ and $\theta(\omega)$, from which $\theta(\omega)$ is found:

$$\ln r(\omega) = \frac{2}{\pi} \int_0^\infty \frac{\omega'\theta(\omega') - \omega\theta(\omega)}{\omega'^2 - \omega^2} d\omega' \tag{6.32}$$

$$\theta(\omega) = -\frac{2\omega}{\pi} \int_0^\infty \frac{\ln r(\omega') - \ln r(\omega)}{\omega'^2 - \omega^2} d\omega'. \tag{6.33}$$

where $\ln \mathcal{R}(\omega) = 2\ln r(\omega)$.

From a knowledge of the frequency dependent reflectivity $\mathcal{R}(\omega)$, the reflection coefficient $r(\omega)$ and the phase of the reflectivity coefficient $\theta(\omega)$ can be found. We can then find the frequency dependence of the optical constants $\tilde{n}(\omega)$ and $\tilde{k}(\omega)$, which in turn yields the frequency dependent dielectric functions $\varepsilon_1(\omega)$ and $\varepsilon_2(\omega)$. Starting with the experimental data for the reflectivity $\mathcal{R}(\omega)$ for germanium in Fig. 6.3(a), the Kramers–Kronig relations are used to obtain results for $\varepsilon_1(\omega)$ and $\varepsilon_2(\omega)$ for germanium as shown in Fig. 6.3(b).

The Kramers–Kronig relations for the conjugate variables $\varepsilon_1(\omega)$ and $\varepsilon_2(\omega)$; $\tilde{n}(\omega)$ and $\tilde{k}(\omega)$; and $\ln r(\omega)$ and $\theta(\omega)$ are widely used in quantitative studies of the optical properties of specific materials, as for example germanium in Fig. 6.3.

6.2 Optical Properties and Band Structure

If we are interested in studying the optical properties near the band edge such as the onset of indirect transitions or of the lowest direct interband transitions, then we should carry out absorption measurements (Chapter 5) to determine the absorption coefficient $\alpha_{\text{abs}}(\omega)$ and thus identify the type of process that is dominant (indirect, direct, allowed, forbidden, etc.) at the band edge. However, if we are interested in the optical properties of a semiconductor over a wide energy range, then we want to treat all bands and transitions within a few eV from the Fermi level on an equal footing. Away from the band edge, the absorption coefficients become too high for the absorption technique to be useful, and reflectivity measurements are made instead. Experimentally, it is most convenient to carry out reflectivity measurements at normal incidence. From these measurements, the Kramers–Kronig analysis (see §6.1) is used to get the phase angle $\theta(\omega)$ for some frequency ω_0, if the reflection coefficient $r(\omega)$ is known throughout the entire range of photon energies

$$\theta(\omega_0) = -\frac{2\omega_0}{\pi} \int_0^\infty \frac{\ln r(\omega) - \ln r(\omega_0)}{\omega^2 - \omega_0^2} d\omega. \tag{6.34}$$

From a knowledge of $r(\omega)$ and $\theta(\omega)$, we can then find the frequency dependence of the optical constants $\tilde{n}(\omega)$ and $\tilde{k}(\omega)$ using Eqs. 6.30 and 6.31 and the frequency dependent dielectric function

$$\varepsilon_1(\omega) = \tilde{n}^2 - \tilde{k}^2 \tag{6.35}$$

$$\varepsilon_2(\omega) = 2\tilde{n}\tilde{k}. \tag{6.36}$$

As an example of such an analysis, let us consider the case of the semiconductor germanium. The normal incidence reflectivity is given in Fig. 6.3(a) and the results of the Kramers–Kronig analysis described above are given for $\varepsilon_1(\omega)$ and $\varepsilon_2(\omega)$ in Fig. 6.3(b).

Figure 6.3: (a) Frequency dependence of the reflectivity of Ge over a wide frequency range. (b) Plot of the real $[\varepsilon_1(\omega)]$ and imaginary $[\varepsilon_2(\omega)]$ parts of the dielectric functions for Ge obtained by a Kramers–Kronig analysis of the reflectivity data in part (a).
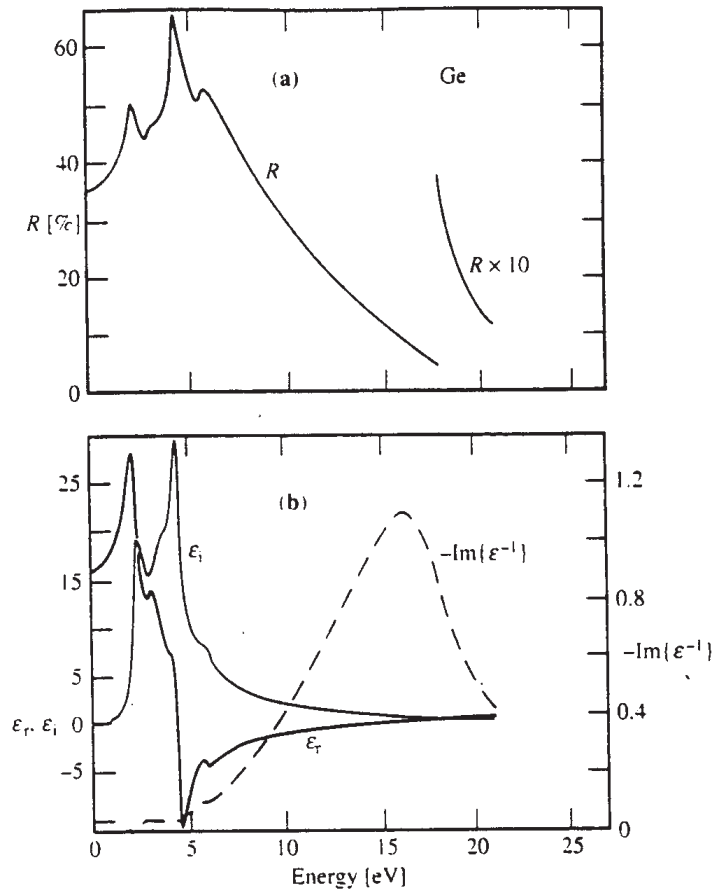
Corresponding to the structure in the reflectivity, there will be structure observed in the real and imaginary parts of the dielectric function. These structures in the reflectivity data are then identified with special features in the energy band structure. It is interesting to note that the indirect transition (0.66 eV) from the $\Gamma_{25'}$ valence band to the L_1 conduction band (see Part I of the notes) has almost no impact on the reflectivity data. Nor does the direct band gap, which is responsible for the fundamental absorption edge in germanium, have a significant effect on the reflectivity data. These effects are small on the scale of the reflectivity structures shown in Fig. 6.3(a) and must be looked for with great care in a narrow frequency range where structure in the absorption data is found. The big contribution to the dielectric constant comes from interband transitions $L_{3'} \rightarrow L_1$ for which the joint density of states is large over large volumes of the Brillouin zone. The sharp rise in $\varepsilon_2(\omega)$ at 2.1 eV is associated with the $L_{3'} \rightarrow L_1$ transition. For higher photon energies, large volumes of the Brillouin zone contribute until a photon energy of about 5 eV is reached. Above this photon energy, we cannot find bands that track each other closely enough to give interband transitions with intensities of large magnitude.

6.3   Modulated Reflectivity Experiments

If we wish to study the *critical point* contributions to the optical reflectivity in more detail, it is useful to carry out modulated reflectivity measurements. If, for example, a small periodic perturbation is applied to a sample then there will be a change in reflectivity at the frequency of that perturbation. The frequency dependence of this change in reflectivity is small (parts in 10^3 or 10^4) but it is measurable. As an example, we show in Fig. 6.4, results for the reflectivity $R(\omega)$ and for the wavelength modulated reflectivity $(1/R)(dR/dE)$ of GaAs. Structure at E_0 would be identified with the direct band gap, while the structure at $E_0 + \Delta_0$ corresponds to a transition from the split-off valence band at $\vec{k} = 0$ which arises through the spin-orbit interaction. The transitions at E_1 and $E_1 + \Delta$ correspond to Λ point and L point transitions, also showing spin-orbit splitting. Also identified in Fig. 6.5 are the $E_{0'}$ transition from the Δ_7 valence band to the Δ_6 conduction band, and the E_2 transition from $X_5 \rightarrow X_5$ at the X point. Although the band structure and notation given in Fig. 6.5 applies to Ge in detail, the results for other group IV and III–V semiconductors is qualitatively similar, with values for the pertinent interband transitions given in Table 6.1 for Si, Ge, GaAs, InP and GaP.

In the vicinity of a critical point, the denominator in the joint density of states is small, so that a small change in photon energy can produce a significant change in the joint density of states. Hence, modulation spectroscopy techniques emphasize critical points. There are a number of parameters that can be varied in these modulation spectroscopy experiments:

electric field	–	electro-reflectance
wavelength	–	wavelength modulation
stress	–	piezoreflectance
light intensity	–	photo-reflectance
temperature	–	thermo-reflectance.

The various modulated reflectivity experiments are complementary rather than yielding identical information. For example, certain structures in the reflectance respond more